



## Analytical solution of nitracline with the evolution of subsurface chlorophyll maximum in stratified water columns

Xiang Gong<sup>1, 2</sup>, Wensheng Jiang<sup>2, 3</sup>, Linhui Wang<sup>2</sup>, Huiwang Gao<sup>2, 4\*</sup>, Emmanuel Boss<sup>5</sup>, Xiaohong Yao<sup>2,4</sup>, Shuh-Ji Kao<sup>6</sup>, Jie Shi<sup>2</sup>

5 <sup>1</sup> School of Mathematics and Physics, Qingdao University of Science and Technology, Qingdao 266061, P. R. China

<sup>2</sup> Key Laboratory of Marine Environment and Ecology (Ministry of Education of China), Ocean University of China, Qingdao 266100, P. R. China

10 <sup>3</sup> Key Laboratory of Physical Oceanography (Ministry of Education of China), Ocean University of China, Qingdao 266100, P. R. China

<sup>4</sup> Qingdao Collaborative Center of Marine Science and Technology, Ocean University of China, Qingdao 266100, P. R. China

<sup>5</sup> School of Marine Sciences, University of Maine, Orono 04469-5706, USA

15 <sup>6</sup> State Key Laboratory of Marine Environmental Science, Xiamen University, Xiamen 361005, P. R. China

\*Corresponding author: Huiwang Gao, hwgao@ouc.edu.cn

### Abstract:

20 In a stratified water column, the nitracline is a layer where the nitrate concentration increases below the nutrient-depleted upper layer, exhibiting a strong vertical gradient in the euphotic zone. The subsurface chlorophyll maximum layer (SCML) forms near the bottom of euphotic zone, acting as a trap to diminish the upward nutrient supply. Depth and steepness of the nitracline are important measurable parameters related to the vertical transport of nitrate into the euphotic zone. The correlation between the  
25 SCML and the nitracline has been widely reported in the literature, but the analytic solution for the relationship between them is not well established. By incorporating a piecewise function for the approximate Gaussian vertical profile of chlorophyll, we derive analytical solutions for the system of phytoplankton and nutrient. The analytical solution shows that the nitracline depth is deeper than the depth of SCML,



30 shoaling with an increase in light attenuation coefficient and with a decrease in  
surface light intensity. The inverse proportional relationship between the light level at  
the nitracline depth and the maximum rate of new primary production is derived,  
suggesting that the light level at the nitracline can be used as an indicator for  
integrated new primary production. Analytic solutions also show that a thinner SCML  
35 corresponds to a steeper nitracline. The nitracline steepness is positively related to  
light attenuation coefficient, but independent of surface light intensity. The derived  
equations of the nitracline in relation to the SCML provide further insight into the  
important role of the nitracline in marine pelagic ecosystems.



## 1 Introduction

40 Nitrogen availability, especially the nitrate upward supply to the euphotic zone where light intensity is sufficient to support net photosynthesis, limits the primary productivity in a stratified water column (Falkowski et al., 1998). Specifically, the nitrate supply from below and the light attenuated from above with the depth collaboratively affect the growth of phytoplankton and lead to the subsurface  
45 chlorophyll maximum (SCM) (Riley et al., 1949; Steele and Yentsch, 1960; Herbland and Voituriez, 1979; Cullen, 1982). The SCM layer (SCML) has attracted much attention since Riley (1949) because the layer contributes significantly to new primary production (NPP) in stratified waters (Probyn et al., 1995; Ross and Sharples, 2007; Fernand et al., 2013). The synergistic physical and biological interaction leads to a  
50 strong vertical nitrate gradient, conventionally referred to as the nitracline (Eppley et al., 1978; Herbland and Voituriez, 1979; Cullen and Eppley, 1981). Depth and steepness of the nitracline are important measurable parameters in regulating the supply of nitrate to the euphotic zone, and hence affecting NPP (Lewis et al., 1986; Bahamón et al., 2003; Aksnes et al., 2007; Cermeno et al., 2008; Omand and  
55 Mahadevan, 2015).

The nitracline depth physically depends on the degree of water column stratification and the magnitude of momentum transfer associated with wind stress (Denman and Gargett, 1983; Laanemets et al., 2004). It also depends on momentum transfer from below (Lipschultz et al., 2002) and in some cases, vertical advection such as  
60 upwelling (Laanemets et al., 2004). However, in a relatively stable environment, the SCML may restrict the diffusive flux of nitrates to the euphotic zone and continually erode the nitracline supposing that sufficient light is available (Probyn et al., 1995). The SCML thereby acts as an effective nutrient trap, regulating the nitracline depth (Banse, 1982; Beckmann and Hense, 2007; Klausmeier and Litchman, 2001; Probyn  
65 et al., 1995). On the other hand, variation of nitracline steepness, which is critical to determine the nitrate supply, was poorly understood due to lack of high vertical resolution data, e.g., both bottle data and Argo data tend to have low vertical



70 resolution sampling. Some studies showed that nitrogen flux is dependent more on the nitracline steepness than on the density gradients regulating turbulent diffusion (Bahamón and Cruzado, 2003; Bahamón et al., 2003; Lavigne et al., 2015). Thus, these measurable features of nitracline and their correlation with SCML may provide insightful information for mechanisms of the productivity in pelagic ecosystem, and the analytic solutions for these parameters may fill the knowledge gap.

75 Although a close relationship between the nitracline and SCML is always observed, the quantitative nature of nitracline in relation to the SCML formation has not been studied. The system of phytoplankton and the limiting nutrient on the vertical axis was often utilized to study the depth, intensity, and persistence of the SCML. Major theoretical results include photoacclimation (increase of chlorophyll per cell) (Steele, 1964; Fennel and Boss, 2003), bistability (Yoshiyama and Nakajima, 2002; Ryabov et al., 2010), oscillating SCM (Huisman et al., 2006), hysteresis conditions (Kiefer and Kremer, 1981; Navarro and Ruiz, 2013), and the ESS (evolutionary stable strategy) depth obtained by game-theory approach (Klausmeier and Litchman, 2001; Mellard et al., 2011). Recent mathematical studies solved the persistence and uniqueness of the steady state solution (Du and Hsu, 2010; Hsu and Yuan, 2010; Du and Mei, 2011), 85 and gave rigorous proofs for the above-mentioned ESS depth and the game-theory approach (Du and Hsu, 2008a, b). Additionally, several modeling studies have been conducted to quantitatively assess the importance of different physic-biological processes leading to SCML (Jamart et al., 1977; Jamart et al., 1979; Varela et al., 1994; Klausmeier and Litchman, 2001; Hodges and Rudnick, 2004; Beckmann and 90 Hense, 2007).

Among the studies using the nutrient-phytoplankton model, Klausmeier and Litchman (2001) first analytically derived the vertical nutrient distribution with the development of the SCML. In that model, the concentration of the limiting nutrient was found to be low and constant above the SCML and linearly increasing with depth 95 below this layer in poorly mixed water column. Building on that model, Mellard et al. (2011) added stratification and surface nutrient input, which can make phytoplankton



grow in both the surface mixed layer and deep layer (SCML) simultaneously. Fennel and Boss (2003) derived that the sum of nutrients and phytoplankton at steady state will increase monotonically below the surface mixed layer until it equals the fixed nutrient concentration. By incorporating a generalized Gaussian function for vertical chlorophyll profile into the nutrient-phytoplankton dynamic equation, Gong et al. (2015) obtained that the steady-state nitrate concentration increased from the upper community compensation depth to the SCML depth. None of the studies, however, focused on the quantitative nature of nitracline in relation to the SCML in the stratified waters.

In this paper, we modified the nutrient-phytoplankton model by Gong et al. (2015) to study the roles of SCM in reshaping the nitracline. Two additional terms, atmospheric input, which promotes the growth of phytoplankton in the surface mixed layer, and the phytoplankton self-shading, which regulates the light penetration, were introduced into the previous model. Accordingly, a piecewise function comprising a constant value within the surface mixed layer and a Gaussian function below this layer was used to fit vertical chlorophyll profiles. We derived the analytic solutions for the properties of the nitracline and the SCML in steady state, respectively, and the relationship between them was examined in response to light availability, surface nutrient input, and vertical diffusivity.

## 2 Definitions and Models

### 2.1 Models

#### 2.1.1 Dynamic equations

We consider the following equations for phytoplankton and nutrient dynamics in stratified waters (Eqs. 1-2), where light and nitrogen are two limiting factors for phytoplankton growth (Fig. 1). The change in phytoplankton at depth  $z$  is the balance of the growth and death, and the passive moving (sinking and mixing) (Eq. 1). An eddy diffusion coefficient  $K_v$  redistributes phytoplankton in the water column. Depth  $z$  is increasing toward the seabed.



$$\begin{cases}
 \frac{\partial P}{\partial t} = \mu_m \min(f(I), g(N))P - \varepsilon P - w \frac{\partial P}{\partial z} + \frac{\partial}{\partial z} \left( K_v(z) \frac{\partial P}{\partial z} \right) & (1) \\
 \frac{\partial N}{\partial t} = -\gamma \mu_m \min(f(I), g(N))P + \gamma \alpha \varepsilon P + N_{in}(z) + \frac{\partial}{\partial z} \left( K_v(z) \frac{\partial N}{\partial z} \right) & (2)
 \end{cases}$$

where  $P$  denotes the chlorophyll concentration ( $\text{mg m}^{-3}$ ). We assume the chlorophyll distribution to represent the distribution of phytoplankton biomass (that means that the photoacclimation of phytoplankton is ignored, and the SCM refers to the subsurface biomass maximum, SBM). This is a significant simplification. In fact, phytoplankton increases inter-cellular pigment concentration when light level decreases (Cullen, 1982; Fennel and Boss, 2003; Cullen, 2015). The presence of a SBM layer does typically imply a SCML, and any mechanism that causes the former also causes the latter (Hodges and Rudnick, 2004). Usually, the depths of SCML and SBML are separate, and the latter is shallower than the former.

Nitrogen  $N$  (in unit:  $\text{mmol N m}^{-3}$ ) taken up by phytoplankton includes three sources, i.e., recycling from dead phytoplankton, atmospheric input to the surface mixed layer, and supply by mixing from deep water (Eq. 2).  $\gamma$  is the nitrogen content of the phytoplankton ( $\text{mmol N per mg Chl}$ ). Following Mellard et al. (2011), we consider the nitrogen input from atmosphere at the rate of  $N_{in}(z)$ , setting as a delta function at  $z=0$  with the total nutrient input in the surface mixed layer  $N_{inML}$ ,  $N_{inML} = \int_0^{z_s} N_{in}(z) dz$ , where  $z_s$  is the depth of surface mixed layer. Note that nitrogen input through the activity of nitrogen fixers is excluded. However, trichodesmium, if they are a mat at the surface, will be modeled similarly to the atmospheric input term.

$\mu_m$  is the maximum growth rate of phytoplankton,  $\varepsilon$  is the loss rate of phytoplankton (including respiration, mortality, zooplankton grazing), and  $\alpha$  is the recycling rate of dead phytoplankton ( $0 < \alpha < 1$ ). The specific rate of loss processes ( $\varepsilon$ ) is assumed to be vertically homogeneous due to lack of data (similar to Sverdrup, 1953). The treatment of grazing loss, is, in the least, an oversimplification, though many numerical models used a similar one (e.g., Klausmeier and Litchman, 2001; Fennel and Boss, 2003; Huisman et al., 2006). The growth-limited function for light  $I$  and nitrogen  $N$  is given



by  $\mu_m \min(f(I), g(N))$ . The Michaelis-Menten form for the light-limiting function  $f(I)$  and nitrogen-limiting function  $g(N)$ ,  $f(I) = I/(K_I + I)$  and  $g(N) = N/(K_N + N)$  is used, where  $K_I$  and  $K_N$  denote the half-saturation constants for light and nitrogen, respectively. The net growth rate,  $\mu_m \min(f(I), g(N)) - \varepsilon$ , is positive only if both light-limiting term  
 155  $\mu_m f(I)$  and nitrogen-limiting term  $\mu_m g(N)$  are larger than the loss rate  $\varepsilon$ .

Light intensity  $I$  decreases exponentially with depth according to the Lambert-Beer law,

$$I(z) = I_0 \exp\left(-K_w z - K_c \int_0^z P dz\right) \quad (3)$$

where  $I_0$  is the surface light intensity,  $K_w$  and  $K_c$  are light attenuation coefficients of  
 160 water and phytoplankton, respectively. For the sake of simplicity, we assume that both  $K_w$  and  $K_c$  are constant with depth.

The sinking velocity of phytoplankton  $w$  is non-negative in the chosen coordinate system. We assumed it to be constant with depths, neglecting the influencing of density gradients (pycnoclines), which may cause vertical variations in sinking.

165 To describe the water column stratification, we assume that the vertical eddy diffusivity  $K_v$  depends on depths,

$$K_v(z) = \begin{cases} K_{v1} & 0 \leq z \leq z_s \\ K_{v2} & z_s < z < z_b \end{cases} \quad (4)$$

where  $z_b$  is set to the bottom boundary of this model and is assumed to be sufficiently deep where the chlorophyll concentration approaches to zero. We assume that surface  
 170 diffusivity ( $K_{v1}$ ) and subsurface diffusivity ( $K_{v2}$ ) (Lande and Wood, 1987; Hodges and Rudnick, 2004) are constant and  $K_{v1}$  is large enough to homogenize the chlorophyll and nitrogen concentration in the surface mixed layer. A gradual transition from the surface mixed layer to the deep one (in the vicinity of  $z_s$ ) can be written in terms of a generalized Fermi function (Ryabov et al., 2010),  $K_v(z) = K_{v2} + \frac{K_{v1} - K_{v2}}{1 + e^{z - z_s/l}}$ , where  
 175 parameter  $l$  characterizes the width of the transition layer. In our numerical study, we assumed this transition layer is 2 m. For simplicity, parameter  $l$  is set to infinitely thin



in analytic solutions. A comprehensive list of symbols is given in Table 1.

The zero-flux boundary condition for the phytoplankton at the surface is used. At the bottom boundary of the model domain ( $z=z_b$ ) the Dirichlet boundary condition is used, i.e.,  $P \rightarrow 0$  for  $z \rightarrow z_b$ . Fennel and Boss (2003) used an infinite depth as  $z_b$  ( $z_b \rightarrow \infty$ ). For the nitrogen distribution we set  $N=N_{inML}$  at the surface and diffusing into the water column a prescribed nitrate gradient,  $n$ , at the bottom. That is,

$$\begin{cases} \left( wP - K_{v1} \frac{\partial P}{\partial z} \right) \Big|_{z=0} = 0, & P(z_b) = 0. \\ N \Big|_{z=0} = N_{inML}, & \frac{\partial N}{\partial z} \Big|_{z=z_b} = n. \end{cases} \quad (5)$$

### 2.1.2 Fitting equation for vertical chlorophyll profile

In many stratified water columns, the vertical distribution of chlorophyll concentration is homogeneous within the surface mixed layer and appears a Gaussian below this layer (Fig. 2a), which is typical in open oceans (Uitz et al., 2006), shelf seas (Sharples et al., 2001), stratified estuary (Lund-Hansen, 2011), and arctic waters (Martin et al., 2012). The non-uniform vertical profile of chlorophyll with an SCML was first modeled by a generalized Gaussian function (Lewis et al., 1983), which has subsequently been widely used with small modifications. For example, Platt et al. (1988) superimposed a constant background on the generalized Gaussian, and fitted it to field data on the vertical distribution of chlorophyll from coastal, upwelling, open oceans and Arctic waters. Afterward, some studies introduced a parameter to represent the slope of the Gaussian curve (Matsumura and Shiomoto, 1993; Mu Oz Anderson et al., 2015). In particular, to account for the observed characteristic that surface values always exceed the bottom ones (Fig. 2a), the generalized Gaussian functional form has been modified with a superimposition of a background linearly or exponentially decreasing with depth (Uitz et al., 2006; Mignot et al., 2011; Ardyna et al., 2013).

For simplicity, to analytically study the role of the SCML on shaping the nitracline, we therefore propose a piecewise function comprising a constant value in the surface mixed layer and below a general Gaussian function (Eq. 6) to approximate the vertical





profile of chlorophyll concentration in Fig. 2a.

$$P = \begin{cases} P_0 & 0 \leq z \leq z_s \\ P_{\max} \exp\left[-\frac{(z-z_m)^2}{2\sigma^2}\right] & z_s < z < z_b \end{cases} \quad (6)$$

205 where  $P$  is chlorophyll concentration as a function of depth  $z$ ,  $P_0$  is the chlorophyll concentration within the surface mixed layer, and  $P_{\max} = h/(\sigma\sqrt{2\pi})$  represents the maximum value of chlorophyll below the surface mixed layer. Note that the vertical distribution of chlorophyll is an incomplete general Gaussian function below the surface mixed layer (see Fig. 2a). The three Gaussian parameters ( $P_{\max}$ ,  $z_m$ ,  $\sigma$ ) can

210 characterize the SCM phenomenon. Thus,  $z_m$  is the depth of the maximum chlorophyll (the peak of the bell shape), and  $\sigma$  is the standard deviation of Gaussian function, which controls the width of the SCML. The upper and lower boundary of SCML can be defined as  $z_m - \sigma$  and  $z_m + \sigma$ , respectively, which are at the depths where there is the balance between phytoplankton growth and losses and thus reflect the

215 physical-biological ecosystem dynamics associated with SCML (Beckmann and Hense, 2007; Gong et al., 2015). To explore the SCML in stratified waters, we assume the surface mixed layer is shallower than the upper boundary of the SCML, i.e.,  $z_s < z_m - \sigma$ . Examples of the piecewise function that reasonably well fitted to vertical chlorophyll profiles in the northern South China Sea (SCS) can be found in Gong et al.

220 (2014).

Considering the influence of the surface mixed layer on the chlorophyll vertical distribution,  $h$  is less than the total chlorophyll concentration integrated through the water column. We assume  $\lambda h$  ( $\text{mg}/\text{m}^2$ ) is the integrated chlorophyll concentration below the surface mixed layer. Based on the properties of Gaussian function,  $\lambda$  can be

225 expressed as  $\lambda = \Phi\left(\frac{z_b - z_m}{\sigma}\right) - \Phi\left(\frac{z_s - z_m}{\sigma}\right)$ , where  $\Phi\left(\frac{z_b - z_m}{\sigma}\right)$  and  $\Phi\left(\frac{z_s - z_m}{\sigma}\right)$  can be obtained from the standard normal table. According to the property of Gaussian function, we have  $0.68 < \lambda < 1.00$ ,  $z_s < z < z_b$ , under the assumption of  $z_s < z_m - \sigma$ .



The piecewise function approximation (Eq. 6) was evaluated and justified through numerical simulation of the nutrient-phytoplankton system (Eqs. 1-2), which is solved  
230 with a semi-implicit time stepping scheme. The vertical resolution is uniform (2 m), extending down to 200 m. We assumed a small uniformly distributed concentration of phytoplankton ( $P(z,0)=0.1 \text{ mg m}^{-3}$ ) and nitrogen ( $N(z,0)=0.1 \text{ mmol N m}^{-3}$ ) as the initial conditions and run the model until in converge to a steady state (The modeling results show that the steady state has no relationship with the initial values of  
235 phytoplankton and nitrogen). We use the biologically reasonable parameter values given in Table 1 to represent the system at Station SEATS (South East Asia Time Series) in the northern SCS.

Fig. 3 shows the numerically simulated equilibrium distributions of nitrogen, light, and chlorophyll. In addition, the simulated vertical profile of chlorophyll is fitted well  
240 by the piecewise function of chlorophyll using the least square method (Fig. 3). Many numerical solutions of the nutrient-phytoplankton system have reproduced the vertical chlorophyll profile with the SCML (Fennel and Boss, 2003; Huisman et al., 2006; Ryabov et al., 2010). Thus, analogous to the study by Klausmeier and Litchman (2001), we incorporate the piecewise function (Eq. 6) to the nutrient-phytoplankton  
245 system (Eqs. 1-2) at steady state to examine the roles of the SCML in reshaping the nitracline. We note that the useful delta function approximation in Klausmeier and Litchman (2001) was verified by both simulation and rigorous mathematics (Du and Hsu, 2008a, b). As presented above, the assumption of the piecewise function approximation is physically practical.

## 250 2.2 Definition of the nitracline

The vertical distributions of nitrate often exhibit a strong gradient in depth (the nitracline), but the feature of nitracline (depth, steepness) is variable in euphotic zones due to the combined effect of physical and biological processes.

Many studies define the nitracline depth as the location where the maximum  
255 vertical gradient in nitrate concentrations occurs (Eppley et al., 1979; Bahamón et al.,



2003; Wong et al., 2007; Beckmann and Hense, 2007; Martin et al., 2010). To measure the defined depth, a high vertical resolution of nitrate concentrations is needed and this is a big technique challenge existing for a long time. Thus, some definitions were also proposed to make the depth measurable. For example, one definition is the depth where the nitrate concentration reaches a prescribed concentration, e.g., 0.05, 0.1, 1.0, or 12 mmol N m<sup>-3</sup> (Cullen and Eppley, 1981; Koeve et al., 1993; Martin and Pondaven, 2003). Some studies choose it to be the first depth where nitrogen is detectable (e.g., 0.05 or 0.1 mmol N m<sup>-3</sup>) (Cermeno et al., 2008; Hickman et al., 2012) or where the nitrogen concentration exceeds the mixed layer value by a prescribed concentration difference (e.g., 0.05 mmol N m<sup>-3</sup>) (Laanemets et al., 2004). Significant differences exist between these defined depths, i.e., the depth of maximal nitrate gradient was found to be deeper by 10 m from the first depth where nitrate can be detected (Eppley et al., 1978), while the nitrate gradient at the first detectable depth of nitrate is nearly zero (Cermeno et al., 2008).

270 With the development of nearly continuous nitrate profile measurement using the In Situ Ultraviolet Spectrophotometer (ISUS) optical nitrate sensor (Johnson and Coletti, 2002; Johnson et al., 2010), the detection of the maximum nitrate gradient could be more accurate than before. In this study, we adopt the depth of the maximum nitrate gradient in the euphotic zone as the nitracline depth ( $z_n$ ), where  $\frac{d^2 N}{dz^2} \Big|_{z_n} = 0$  and

$$275 \quad \frac{d^3 N}{dz^3} \Big|_{z_n} < 0.$$

Below the surface mixed layer, the steady-state version of Eq. (2) reduces to  $\gamma \mu_m \min(f(I), g(N)) P - \gamma \alpha \varepsilon P = K_{v2} \frac{d^2 N}{dz^2}$ . Thus, at the nitracline depth the balance between uptake and recycling terms can be derived:  $\mu_m \min(f(I), g(N)) = \alpha \varepsilon$ .

The nitracline steepness is defined as the nitrate gradient at the nitracline depth  $\left(\frac{dN}{dz} \Big|_{z_n}\right)$  in this study (Laanemets et al., 2004; Aksnes et al., 2007).

### 2.3 Data sources



The nitrate profiles were obtained from the ISUS measurement at the SEATS station during the CHOICE-C 2012 summer cruise. 9 casts were conducted during Aug. 6-7, 2012. The raw ISUS nitrate data, which employed temperature-compensation, were first calibrated by the AutoAnalyzer 3 (AA3), and then smoothed to remove noise (the sampling frequency was set at 5 Hz, thus, the raw data were smoothed with a 5-point moving average, then interpolated by cubic spline function). The corresponding temperature was obtained from Conductivity-Temperature-Depth (CTD) measurements. Overall, nine sets of profiles are available to examine our analytical solutions.

### 3 Results

#### 3.1 Relations between nitracline and SCML

##### 3.1.1 Nitracline depth and SCML

At steady state, multiplying Eq. (1) by  $\gamma$  then adding Eqs. (1) and (2) leads to:

$$(\alpha - 1)\varepsilon P - w \frac{dP}{dz} + \frac{d}{dz} \left( K_v(z) \frac{dP}{dz} \right) + \frac{1}{\gamma} \frac{d}{dz} \left( K_v(z) \frac{dN}{dz} \right) + \frac{N_m(z)}{\gamma} = 0 \quad (7)$$

By substituting the expression of eddy diffusivity (Eq. 4) and the fitted function of chlorophyll (Eq. 6) into Eq. (7), we obtain the diffusive term of nitrate below the surface mixed layer, that is,

$$K_{v2} \frac{d^2 N}{dz^2} = \left[ -\frac{K_{v2}}{\sigma^2} \left( \frac{z - z_m}{\sigma} \right)^2 - \frac{w}{\sigma} \left( \frac{z - z_m}{\sigma} \right) + \frac{K_{v2}}{\sigma^2} + (1 - \alpha)\varepsilon \right] \gamma P \quad (8)$$

Letting  $d^2 N / dz^2 = 0$  in Eq. (8), for  $P > 0$  one gets

$$-\frac{K_{v2}}{\sigma^2} \left( \frac{z - z_m}{\sigma} \right)^2 - \frac{w}{\sigma} \left( \frac{z - z_m}{\sigma} \right) + \frac{K_{v2}}{\sigma^2} + (1 - \alpha)\varepsilon = 0 \quad (9)$$

Solving this quadratic equation of depth  $z$ , we obtain the depths  $z_{n1}$  and  $z_{n2}$ ,



$$\begin{cases} z_{n1} = z_m - \frac{w\sigma^2}{2K_{v2}} - \sqrt{\frac{w^2\sigma^4}{4K_{v2}^2} + \frac{(1-\alpha)\varepsilon\sigma^4}{K_{v2}} + \sigma^2} \\ z_{n2} = z_m - \frac{w\sigma^2}{2K_{v2}} + \sqrt{\frac{w^2\sigma^4}{4K_{v2}^2} + \frac{(1-\alpha)\varepsilon\sigma^4}{K_{v2}} + \sigma^2} \end{cases} \quad (10)$$

Taking the derivative of Eq. (8) with respect to depth  $z$ , we get  
 305  $K_{v2} \frac{d^3N}{dz^3} = \left[ -\frac{2K_{v2}}{\sigma^4}(z-z_m) - \frac{w}{\sigma^2} \right] \gamma P - K_{v2} \frac{d^2N}{dz^2} \frac{z-z_m}{\sigma^2}$ . Obviously, at depth  $z_{n1}$ ,  $d^3N/dz^3 > 0$ ,  
 and at depth  $z_{n2}$ ,  $d^3N/dz^3 < 0$ . That is,  $z_{n2}$  is the location of maximum nitrate gradients.  
 We obtain that the nitracline depth refers to the depth  $z_{n2}$ , i.e.,

$$z_n = z_{n2} = z_m - \frac{w\sigma^2}{2K_{v2}} + \sqrt{\frac{w^2\sigma^4}{4K_{v2}^2} + \frac{(1-\alpha)\varepsilon\sigma^4}{K_{v2}} + \sigma^2} \quad (11)$$

Particularly, Eq. (9) became a linear function of depth  $z$  when the second order item  
 310 coefficient ( $-K_{v2}/\sigma^4$ ) is zero, thus has only one solution. In fact, in typical stratified  
 waters the diffusivity below the surface mixed layer ( $-K_{v2}$ ) is  $1.9 \times 10^{-5} \text{ m}^2 \text{ s}^{-1}$ , and the  
 thickness of SCML ( $2\sigma$ ) is from several meters to tens of meters (Cullen, 2015), thus,  
 $-K_{v2}/\sigma^4$  (values from  $8.64 \times 10^{-9}$  to  $7.78 \text{ m}^2 \text{ s}^{-1}$ ) can be neglected in some cases. When  
 $-K_{v2}/\sigma^4 \rightarrow 0$ , we get one solution from Eq. (9),

$$315 \quad z_n = z_m + \frac{(1-\alpha)\varepsilon\sigma^2}{w} \quad (12)$$

Both Eqs. (11) and (12) show that the nitracline depth is located below the SCML  
 depth, i.e.,  $z_n > z_m$  (Fig. 1). A numerical study in weak vertical mixing environments  
 showed a similar result (Beckmann and Hense, 2007). Note that the SCML represents  
 the SBML in our model. In some oligotrophic oceans, the SCML will be deeper than  
 320 the SBML due to the effect of photoacclimation on the vertical distribution of  
 chlorophyll (Fennel and Boss, 2003). For example, Li et al. (2015) showed that the  
 modeled maximum nitrate gradient (nitracline) occurred below the depth of SCML in  
 the northern SCS, and then we can deduce that the nitracline depth is also deeper than  
 the depth of SBML. In the Mediterranean Sea, Bahamón et al. (2003) found that the



325 nitracline occurred below the depth of SCML at 88% of the stations (50 out of 57  
 stations). As well known, the SCML in the Mediterranean is often due to  
 photoacclimation. It is not surprised for the other 7 stations against  $z_n > z_m$  in the  
 Mediterranean Sea if photoacclimation leads to a much deeper SCML than the SBML.  
 Thus, we conclude that the nitracline depth is located below the SBML depth, while  
 330 the locations may not be necessarily true between the depths of nitracline and SCML.

### 3.2.2 Nitracline steepness and SCML

To illustrate the relationship between the nitracline steepness and the SCML, by  
 integrating Eq. (8) from depth  $z_n$  to  $z_b$  and using the assumption for phytoplankton at  
 the bottom boundary, i.e.,  $P \rightarrow 0$  for  $z \rightarrow z_b$  (Eq. 5), we get

$$335 \quad \left. \frac{dN}{dz} \right|_{z_n} = \left( \frac{z_n - z_m - \frac{w}{K_{v2}}}{\sigma^2} \right) \gamma P \Big|_{z_n} + \frac{(1-\alpha)\varepsilon\gamma}{K_{v2}} \int_{z_n}^{z_b} P dz \quad (13)$$

This equality indicates that the nitracline gets steeper as the distance between the  
 depths of nitracline layer and SCML is increased.

Incorporating Eq. (11) into Eq. (13) leads to

$$\left. \frac{dN}{dz} \right|_{z_n} = \left( \sqrt{\frac{w^2}{4K_{v2}^2} + \frac{(1-\alpha)\varepsilon}{K_{v2}} + \frac{1}{\sigma^2}} - \frac{3w}{2K_{v2}} \right) \gamma P \Big|_{z_n} + \frac{(1-\alpha)\varepsilon\gamma}{K_{v2}} \int_{z_n}^{z_b} P dz \quad (14)$$

340 Equation (14) indicates that the nitracline steepness is negatively related to the  
 thickness of SCML.

## 3.2 Analytical solutions for nitracline features

### 3.2.1 Depth of the nitracline

By substituting the general Gaussian function for chlorophyll below the surface  
 345 mixed layer (Eq. 6) into Eq. (1), we obtain the steady-state net growth rate of  
 phytoplankton below the surface mixed layer:

$$\mu_m \min(f(I), g(N)) - \varepsilon = -K_{v2} \left( z - \left( z_m - \frac{w\sigma^2}{2K_{v2}} \right) \right)^2 / \left( \sigma^4 + w^2/4K_{v2} + K_{v2}/\sigma^2 \right) \quad (15)$$



Let  $z_0 = z_m - w\sigma^2 / (2K_{v2})$  in the first term of the right-hand of Eq. (15). From the result given by Gong et al. (2015), we know that  $z_0$  is the location of the maximum growth rate of phytoplankton (hereafter named as the depth of optimal growth), where the transition from nutrients limitation to light limitation occurs (i.e.,  $f(I)=g(N)$  at depth  $z_0$ ).

Clearly,  $z_n > z_0$  (Eq. 11). Hence, the growth of phytoplankton at the nitracline depth  $z_n$  is limited by light, i.e.,  $\mu_m \min(f(I), g(N))|_{z_n} = \mu_m f(I)|_{z_n}$ . In other words, the growth rate of phytoplankton at the nitracline depth is a function of the light level at the nitracline depth,  $I(z_n)$ . Thus, from Eqs. (11) and (15), we obtain the growth rate of phytoplankton at the nitracline depth, that is,

$$\mu_m f(I)|_{z_n} = \alpha \varepsilon \quad (16)$$

Substituting the Michaelis-Menten form for  $f(I)$  into Eq. (16), we have

$$I(z_n) = \frac{K_I}{\mu_m / \alpha \varepsilon - 1} \quad (17)$$

Rearranging Eq. (17), we find  $\mu_m - \alpha \varepsilon = \alpha \varepsilon K_I / I(z_n)$ . This equality indicates that the maximum rate of NPP,  $(\mu_m - \alpha \varepsilon)P$ , is inversely proportional to the light level at the nitracline depth,  $I(z_n)$ . It follows that the light level at the nitracline depth is an indicator of integrated NPP in water columns.

Furthermore, insertion of Eq. (3) into Eq. (17) yields another expression of the nitracline depth:

$$z_n = \frac{1}{K_w} \ln \frac{I_0 (\mu_m / \alpha \varepsilon - 1)}{K_I} - \frac{\gamma}{K_w} K_c \int_0^{z_n} P dz \quad (18)$$

Note that Eq. (18) is obtained on the premise that the nitracline depth exists. This equality shows that the nitracline depth is inversely proportional to the light attenuation coefficient of water ( $K_w$ ), and it deepens logarithmically with increasing surface light intensity ( $I_0$ ). It is noted that the nitracline depth has a negative relation



with the self-shading of phytoplankton ( $K_c \int_0^{z_n} P dz$ ).

Importantly, Eq. (18) predicts that the nitracline depth has no relation with subsurface diffusivity. Aksnes et al. (2007) also proposed a similar result that a shoaling nitracline per se cannot be taken as an unequivocal sign of increased upwelling, as well as eddy diffusion. However, this does not mean that fluid dynamics are unimportant in shaping vertical distribution of nitrate. Equation (18) also indicates that both a higher recycling rate ( $\alpha$ ) of dead phytoplankton and a larger loss rate ( $\epsilon$ ) lead to a shallower nitracline, while the enhanced maximum growth rate of phytoplankton ( $\mu_m$ ) moves the nitracline depth downward.

### 3.2.2 Steepness of the nitracline

In steady state, integrating Eq. (2) from the nitracline depth  $z_n$  to the bottom boundary  $z_b$ , and considering the light limitation of phytoplankton growth below depth  $z_n$  (Eq. 15), we obtain the nitrate gradient below the surface mixed layer,

$$\frac{dN}{dz} \Big|_{z_n} = n + \frac{1}{K_{v2}} \int_{z_n}^{z_b} (\alpha \epsilon - \mu_m f(I)) \gamma P dz \quad (19)$$

This equality shows that the nitracline steepness enhances with increasing nitrate gradient at the bottom boundary ( $n = \frac{dN}{dz} \Big|_{z_b}$ ) which depends on the intensity of nitrate intrusion from below. The vertical diffusion negatively influences the nitracline steepness. The modeled time-series distributions of nitrate gradients and diffusive nitrate fluxes in the northern SCS and the upstream Kuroshio Current showed similar results (Li et al., 2015). Beckmann and Hense (2007) conducted sensitivity analysis of both vertical diffusivity and nutrient concentration at the bottom boundary to examine the vertical phytoplankton and nutrient profiles in oligotrophic oceans and their numerical results support the relations presented in Eq. (19).

### 3.3 Analytical solutions for SCM characteristics

Similar to methods used by Gong et al. (2015), the piecewise function for vertical chlorophyll profile (Eq. 6) was incorporated into the nutrient-phytoplankton model





(Eqs. 1-2) at steady state to derive the three SCM characteristics (SCML thickness, its depth and intensity).

400 For  $z = z_m$  and  $z = z_m + \sigma$ , the net growth rate of phytoplankton (Eq. 15) can be respectively expressed as following:

$$\mu_m f(I)|_{z=z_m} - \varepsilon = K_{v2}/\sigma^2 \quad (20)$$

$$\mu_m f(I)|_{z=z_m+\sigma} - \varepsilon = -w/\sigma \quad (21)$$

By substituting the growth limitation function for light to Eq. (20) or Eq. (21), we  
 405 obtain the expression of parameter  $z_m$ , i.e.,

$$z_m = \frac{1}{K_w} \ln \left[ \left( \frac{\mu_m}{\varepsilon + K_{v2}/\sigma^2} - 1 \right) \frac{I_0}{K_l} \right] - \frac{K_c}{K_w} \int_0^{z_m} P dz \quad (22)$$

or

$$z_m = \frac{1}{K_w} \ln \left[ \left( \frac{\mu_m}{\varepsilon - w/\sigma} - 1 \right) \frac{I_0}{K_l} \right] - \frac{K_c}{K_w} \int_0^{z_m+\sigma} P dz - \sigma \quad (23)$$

Subtracting Eqs. (22) and (23), and rearranging, we obtain the expression of  
 410 parameter  $\sigma$ :

$$\left( \frac{\mu_m}{\mu_m - \varepsilon + w/\sigma} - 1 \right) \exp^{K_w \sigma + K_c \int_{z_m}^{z_m+\sigma} P dz} = \frac{\mu_m}{\mu_m - \varepsilon - K_{v2}/\sigma^2} - 1 \quad (24)$$

Neglecting terms including self-shading of phytoplankton ( $K_c$ ) in Eqs. (22-24), both the analytical solutions of the depth and thickness of SCML are the same as the results presented in Gong et al. (2015). The self-shading effect of phytoplankton plays an  
 415 important role in vertical pattern of chlorophyll (Shigesada and Okubo, 1981; Klausmeier and Litchman, 2001; Beckmann and Hense, 2007). Our results indicate that a higher self-shading of phytoplankton negatively influences the depth and thickness of the SCML, having the same effect as an increasing light attenuation coefficient of water,  $K_w$ .



420 The expression of the SCML intensity is also different from the results presented in  
 Gong et al. (2015). Integrating Eq. (7) from the surface of water to the bottom of  
 surface mixed layer ( $z_s$ ), and from the bottom of surface mixed layer to the base of our  
 model domain ( $z_b$ ) respectively, gives:

$$(1-\alpha)\varepsilon\gamma P_0 z_s = K_{v2} \frac{dN}{dz} \Big|_{z_s+0} + N_{inML} \quad (25)$$

425  $(1-\alpha)\varepsilon\gamma\lambda h = K_{v2}n - K_{v2} \frac{dN}{dz} \Big|_{z_s+0} \quad (26)$

Adding Eqs. (25) and (26) yields:

$$(1-\alpha)\varepsilon\gamma(\lambda h + P_0 z_s) = K_{v2}n + N_{inML} \quad (27)$$

Nitrogen input to the surface mixed layer ( $N_{inML}$ ) causes an increase of surface  
 chlorophyll concentration (Eq. 25). Hence, the total chlorophyll in stratified water  
 430 columns ( $\lambda h + P_0 z_s$ ) increases with increasing  $N_{inML}$  (Eq. 27), which has also been  
 predicted by the numerical study (Mellard et al., 2011) and supported by the  
 experimental test (Mellard et al., 2012).

Because recycling processes are assumed to not immediately convert dead  
 phytoplankton back into dissolved nutrients below the surface mixed layer, i.e.,  $\alpha \neq 1$ ,  
 435 the total chlorophyll concentration below the surface mixed layer and the intensity of  
 SCML can be respectively expressed as:

$$\lambda h = \frac{K_{v2}n}{(1-\alpha)\varepsilon\gamma} + \frac{N_{inML} - (1-\alpha)\varepsilon P_0 z_s}{(1-\alpha)\varepsilon\gamma} \quad (28)$$

$$P_{\max} = \frac{1}{\lambda\sqrt{2\pi}\sigma} \left( \frac{K_{v2}n}{(1-\alpha)\varepsilon\gamma} + \frac{N_{inML} - (1-\alpha)\varepsilon P_0 z_s}{(1-\alpha)\varepsilon\gamma} \right) \quad (29)$$

The integrated chlorophyll concentration below the surface mixed layer ( $\lambda h$ ) and the  
 440 intensity of SCML ( $P_{\max}$ ) are influenced by  $N_{inML}$  positively and by  $P_0$  negatively (Eqs.  
 28-29). That is to say, the influence of nitrate input to the surface mixed layer on the  
 SCML intensity (also on the integrated chlorophyll concentration below the surface



mixed layer) is non-linear. Hence, their changes ( $\lambda h$  and  $P_{\max}$ ) with varying  $N_{inML}$  cannot be obtained from the steady-state solutions straight forwardly, depending on  
 445 the specific parameter combinations in the model. For example,  $\lambda h$  and  $P_{\max}$  decrease when increasing nutrient enrichment directly to the surface mixed layer in the ecosystem given by Mellard et al. (2011), while they are nearly unchanged in oligotrophic oceans (Varela et al., 1994).

Our results (Eqs. 28-29) also show that enhanced subsurface diffusivity ( $K_{v2}$ )  
 450 increases the integrated chlorophyll concentration and the intensity of the SCML ( $\lambda h$  and  $P_{\max}$ ), as a result of a higher nitrate flux ( $K_{v2}n$ ). Physical upward transport of nitrate across the bottom of nitracline is indeed the main nitrogen source for NPP in the euphotic zone (Ward et al., 1989).

## 4 Discussion

### 4.1 Light effects on nitracline with SCML

We now examine how the steady state nitracline in relate to SCML depends on light availability, especially light level at the nitracline depth.

The light level at the nitracline depth is inversely related to the maximum rate of NPP (Eq. 17). Lande et al. (1989) also found that higher maximum rates of population  
 460 growth corresponded to shallower nitracline depths in the central North Atlantic. This result suggested that the light level at the nitracline depth could be an indicator of integrated NPP.

Substituting Eq. (17) to Eq. (28) and rearranging, we have

$$\frac{K_{v2}n + N_{inML}}{\lambda h + P_0 z_s} = \varepsilon \gamma - \frac{\mu_m \gamma}{K_I / I(z_n) + 1} \quad (30)$$

465 This equality indicates that the light level at the nitracline depth,  $I(z_n)$ , is positively related to the integrated chlorophyll concentration in the whole water column,  $\lambda h + P_0 z_s$ . we can derive from Eq. (3) that the nitracline depth ( $z_n$ ) is inversely related to integrated chlorophyll. This inverse relationship has been observed in many regions.



In southern California coastal waters, the phytoplankton standing stock and its  
470 primary production rate were positively related to the reciprocal nitracline depth  
(Eppley et al., 1978; Eppley et al., 1979). Bahamón et al. (2003) found that larger  
depth-integrated chlorophyll with an average deeper SCML and nitracline (~129m,  
~136m, respectively) occurred in the Western Sargasso, Central Sargasso and Eastern  
Atlantic, compared with that in the Canary Current zone.

475 The nitracline depth deepens with increasing surface light intensity but with  
decreasing light attenuation coefficients ( $K_w$  and  $K_c$ ). These results were consistent  
with observations, e.g., Letelier et al. (2004) found the depth of the nitracline to  
coincide with an isolume, a depth of constant light level in the North Pacific  
Subtropical Gyre.

480 The predicted effect of surface light intensity and light attenuation coefficient on  
the nitracline depth (Eq. 18) implies that the nitracline depth in stratified waters may  
have seasonal variations. In the North Pacific Subtropical Gyre, Letelier et al. (2004)  
found that the nitracline depth differences between winter and summer disappeared  
when nitrate concentrations were plotted against light level in the water column.  
485 Aksnes et al. (2007) found that the seasonal pattern of nitracline depth was governed  
by seasonality in light attenuation coefficient, rather than in surface light intensity.  
Particularly, the inverse proportional relationship between the nitracline depth and  
light attenuation coefficient (Eq. 18) has also been derived from a steady-state model  
by Aksnes et al. (2007), which is consistent with observations in the coastal upwelling  
490 region off Southern California (Aksnes et al., 2007). Tiera et al. (2005) found a  
significant positive correlation between the nitracline depth and the depth of 1%  
surface light intensity (the proportion of reciprocal light attenuation coefficient) in the  
Eastern North Atlantic Subtropical Gyre. Bahamón et al. (2003) showed that the  
nitracline depth remained relatively constant around 1% surface light intensity depth  
495 in Western Sargasso.

The nitracline steepens with a higher light attenuation coefficient ( $K_w$  and  $K_c$ ) due to  
 $K_w$  and  $K_c$  negatively influencing SCML thickness (Eqs. 14 and 25). Numerical



modeling showed that a higher  $K_w$  leads to a thinner SCML and thus a steeper  
nitracline layer (Beckmann and Hense, 2007). Aksnes et al. (2007) also found that the  
500 fluctuations in the nitracline steepness were positively correlated with the fluctuations  
in reciprocal Secchi depth (i.e., light attenuation coefficient) in the upwelling area off  
the coast of the Southern California. We further point out that the nitracline steepness  
almost stays constant when changing surface light intensity ( $I_0$ ), because surface light  
intensity has no relation to the SCML thickness (Eq. 25). The sensitivity analysis of a  
505 one-dimensional (vertical) model showed that the vertical nutrient profiles were  
almost paralleling with each other when increasing surface light intensity (Beckmann  
and Hense, 2007).

The inverse effects of light attenuation coefficient on the nitracline steepness and its  
depth imply that the nitracline becomes steeper as the nitracline shoals. Aksnes et al.  
510 (2007) found this consistent pattern in the upwelling area off the coast of the Southern  
California.

#### 4.2 In presence of surface nutrient input

Current evidences and modeling analyses suggest that climate warming will  
increase ocean stratification, and hence reduce nutrient exchange between the ocean  
515 interior and the upper mixed layer (Cermeno et al., 2008; Chavez et al., 2011).  
Therefore, nutrient input directly to the euphotic layer due to atmospheric deposition  
may become a relatively more important nutrient supply mechanism to the euphotic  
layer (Mackey et al., 2010; Okin et al., 2011; Mellard et al., 2011). However, few  
model studies (e.g., Mellard et al. 2011) have explored the influences of external  
520 surface nutrient supply on vertical phytoplankton distribution.

Observations show that an inter-zone exists between the transition of the surface  
mixed layer and the deep layer, where the nutrient gradient equals nearly zero

$\frac{dN}{dz}\Big|_{z_s+0} = 0$  (Fig. 3), leading to the solution in Eq. (26). It follows that the total

chlorophyll in the surface mixed layer depends on the surface nutrient supply ( $N_{inML}$ )



525 (Eq. 26). In this case, if  $N_{inML}$  is negligible, Eq. (26) degenerates to

$$(1-\alpha)\varepsilon\gamma P_0 z_s = 0 \quad (31)$$

In this case, the dead phytoplankton in surface mixed layer must be fully recycled, i.e.,  $\alpha=1$ , in order to sustain the positive chlorophyll concentration ( $P_0>0$ ). In other words, if the dead phytoplankton cannot be fully recycled in the surface mixed layer, external nutrient supply to the layer is needed to fuel the growth of phytoplankton. Thus, the term, external nutrient supply to the surface mixed layer, should be included in the system equations at steady state to make a positive surface chlorophyll concentration. Numerical results by Mallard et al. (2011) also showed that phytoplankton populations can grow in the mixed layer and in the deep layer together, when there is nutrient input directly to the mixed layer.

Accordingly, we treat the vertical phytoplankton distribution as a piecewise function, comprised by a linear function in the surface mixed layer and a Gaussian function below, which is more realistic than the general Gaussian function. The assumption of the piecewise function for phytoplankton is also consistent with the assumption of piecewise vertical diffusivity. For simplicity, we assume that the transition layer between the surface mixed layer and the deep one is infinitely thin, and the chlorophyll is continuous within the transition layer. By assuming the SCML depth is significantly deeper than the base of the surface mixed layer, we obtain the steady state solutions for the SCML depth and thickness, similar to the solutions using the general Gaussian function. However, the intensity of the SCML is affected by surface nutrient supply with an associated positive increase in phytoplankton concentration.

#### 4.3 SCML trapping Nutrient

Indeed, observations and numerical simulations showed that SCML played a role as a nutrient trap in some regions, restricting the diffusive flux of nitrates to the surface mixed layer (Anderson, 1969; Klausmeier and Litchman, 2001; Navarro and Ruiz, 2013).



From Eq. (10), we know  $z_s < z_{n1} < z_0 - \sigma < z_m - \sigma$  (Fig. 1). That is, the SCML occurred below depth  $z_{n1}$ . For  $z_m < z_n$  (Eq. 10), we know that the upward diffusive nitrate concentration is enrichment for phytoplankton growth in the lower part of the SCML ( $z_m < z < z_m + \sigma$ ). To explore the SCML restricting nitrates into the surface mixed layer, next, we examine if the nitrate concentration at depth  $z_{n1}$  above the upper boundary of the SCML ( $z_{n1} < z_m - \sigma$ ) is depleted.

According to the definition of the depth  $z_0$  (where  $f(I) = g(N)$  holds) and  $z_0 > z_{n1}$  (Eq. 10, Fig. 1), we know that the growth of phytoplankton at depth  $z_{n1}$  is nitrate-limited, i.e.,  $\mu_m \min(f(I), g(N))|_{z_{n1}} = \mu_m g(N)|_{z_{n1}}$ . From Eq. (14), we get that at depth  $z_{n1}$ , the growth rate of phytoplankton equals the recycling rate of dead phytoplankton, i.e.,  $\mu_m g(N)|_{z_{n1}} = \alpha \varepsilon$ . Inserting the Michaelis-Menten form for  $g(N)$  into this equality yields:  $N(z_{n1}) = K_N / (\mu_m / \alpha \varepsilon - 1)$ . Phytoplankton maximum growth rates ( $\mu_m$ ) of 0.2 to 1 per day are typical in optical environmental conditions (Banse, 1982; Timmermans et al., 2005). We choose 0.5 per day to illustrate the result. Loss rate ( $\varepsilon$ ), although not well documented, is often quoted as 10% of the growth rate (Parsons et al., 1984). A reasonable choice for the remineralization efficiency seems to be  $\alpha = 0.5$  (Huisman et al., 2006). The typical value of half-saturation constants for nitrate ( $K_N$ ) is between 0.1 and 0.7 mmol N m<sup>-3</sup> in oceans (Eppley et al., 1969). We adopt 0.4 mmol N m<sup>-3</sup>. Thus, we obtain that the nitrate concentration at depth  $z_{n1}$ ,  $N(z_{n1})$ , is equal to 0.03 mmol N m<sup>-3</sup>, a value lower than the detection limit, indicating the depletion of nitrate above depth  $z_{n1}$ .

Because the SCML acts as a nutrient barrier, it is easy to understand that the rate of NPP in the SCML ( $(\mu_m \min(f(I), g(N)) - \alpha \varepsilon)P, z_m - \sigma < z < z_m + \sigma$ ) is positively related to upward nitrate flux that is trapped. This condition can simply be derived by integrating Eq. (2) vertically at steady state, i.e.,  $\int_{z_m - \sigma}^{z_m + \sigma} (\mu_m \min(f(I), g(N)) - \alpha \varepsilon) \gamma P dz = K_{v2} dN/dz|_{z_m - \sigma}^{z_m + \sigma}$ . This result suggests that, the production within the SCML is fuelled mainly, by nitrate and is thus NPP. Because at



580 the nitracline depth the gross growth rate  $\mu_m \min(f(I), g(N))$  equals the recycling of  
 dead phytoplankton  $\alpha \varepsilon$ , for the constant  $\alpha \varepsilon$  we assumed, within the nitracline layer  
 ( $z_{n1} < z_m - \sigma$  and  $z_m < z_{n2}$ ) the nitrate uptake by phytoplankton has to be supplied by the  
 vertical diffusion. Observations also showed that most of the primary production in  
 SCML was supported by nitrate from vertical diffusion, with an average  $f$ -ratio (i.e.,  
 585 relative contribution of the nitrate uptake to the total nitrogen uptake) of  $0.74 \pm 0.26$   
 during early summer in Canadian Arctic waters (Martin et al., 2012).

#### 4.4 Vertical profile of nitrate gradients

From the monotonicity of the quadratic function of depth  $z$  in the left-hand of Eq.  
 (9), we know that  $d^2N/dz^2 < 0$  when  $z_s < z < z_{n1}$  and  $z_{n2} < z < z_b$ , but  $d^2N/dz^2 > 0$  when  
 590  $z_{n1} < z < z_{n2}$ . In other words, the vertical gradient of the nitrate concentration ( $dN/dz$ )  
 decreases with depth on the interval  $(z_s, z_{n1})$ , while increases on the interval  $(z_{n1}, z_{n2})$ ,  
 and then decreases on the interval  $(z_{n2}, z_b)$ . If we consider the distribution of vertical  
 nitrate gradients as continuous across the base of the surface mixed layer, then we get  
 $dN/dz < 0$  for  $z_s < z < z_{n1}$  under the assumptions of the uniform nitrate distribution within  
 595 the surface mixed layer (i.e.,  $dN/dz = 0, 0 < z < z_s$ ). The schematic of vertical profiles of  
 nitrate gradients and chlorophyll concentrations in stratified waters is shown in Fig. 1.

The negative gradient of nitrate below the surface mixed layer ( $dN/dz < 0$  for  
 $z_s < z < z_{n1}$ ) indicates that the nitrate concentration decreases with depth on the interval  
 ( $z_s, z_{n1}$ ). This decreasing nitrate feature has rarely been observed by traditional  
 600 measurements probably due to the technique-limited low resolution. Some float data  
 showed this feature in vertical nitrate profiles, for example, Sakamoto et al. (2009)  
 found it at depths below the base of surface mixed layer (~45-50 m) by the ISUS  
 temperature-compensated data at an eastern Pacific oligotrophic station. Our in situ  
 time series measurements using the ISUS at SEATS station also showed this  
 605 decreasing feature at depths ~25-30 m (Fig. 4). We note that this decreasing nitrate  
 feature will disappear in our derivation if the subsurface vertical diffusion is too weak  
 (Eq. 12) or the surface mixed layer is deeper than depth  $z_{n1}$ . The possible mechanism





deserved to be explored.

#### 4.5 Limitation and application

610 The model in this study integrates a number of physical, chemical, and biological processes that act together to determine the vertical distribution of phytoplankton and nitrate, under the assumption that the system is strictly vertical and in steady state. A few processes such as oxygen status, photoacclimation, luxury uptake of nutrients, phytoplankton motility, concentration-dependent-herbivory, and depth-dependent  
615 herbivory are not included, although they can affect the vertical distribution of phytoplankton and nitrate. Detritus, dissolved organic matter, and zooplankton are not included explicitly, and all loss processes, except sinking, are set to be linearly proportional to phytoplankton. The sinking velocity of phytoplankton is assumed independent on density gradients. Further, the vertical transport of nutrients is only by  
620 eddy diffusion in our model; in reality, nutrients can be supplied by many processes (turbulence, internal waves, storms, slant-wise and vertical convection), especially by upwelling (Katsumi and Hitomi, 2003; Aksnes et al., 2007).

In this study, the sinking velocity of phytoplankton is set independent on nitrate concentration. Vertically-varying sinking velocity have been observed as  
625 physiological response to variations in light or nutrient levels (Steele and Yentsch, 1960; Bienfang and Harrison, 1984; Richardson and Cullen, 1995). The sinking velocity reduced with decreased light level and with increased nutrient concentration, and the resulting divergence in sinking velocity can be large enough to affect the location of the phytoplankton particle maximum. However, numerical results given by  
630 Fennel and Boss (2003) showed analytically that the divergence of the sinking rate contributes to the location of the SBM layer in a significant way only when the divergence in sinking rates occurred above the compensation depth in stable, oligotrophic environments. They also derived that in stable, oligotrophic environments with a predominance of small cells, the biomass maximum is located at  
635 the depth where growth and losses are equal, leaving few influence by sinking divergence.



The piecewise equation (Eq.6) can be used to mimic a large variety of vertical chlorophyll profiles from coastal, upwelling, open oceans and high latitude waters (Fig. 2). For example, for  $z_s > 0$ , when the depth of surface mixed layer equals or is deeper than the depth of SCML, the vertical profiles like Fig. 2b and 2c are often found in well-mixed waters (Uitz et al., 2006). For  $z_s = 0$ , the vertical distribution of chlorophyll concentration (Fig. 2d) can be expressed by a Gaussian function, which is usually found in coastal upwelling waters (Xiu et al., 2008). Particularly, when  $z_s = 0$  and  $z_m = 0$ , the surface bloom occurs (Fig. 2e). In general, the vertical profiles of chlorophyll can be classified into two types, i.e., one peak distribution or uniform distribution in large regions of lakes and oceans (Uitz et al., 2006; Lavigne et al., 2015).

Choosing the values of model parameters represented the system in the northern SCS (given in Table 1), we can retrieve the nitracline depth and steepness, the optimal depth and the three SCM characteristics. To make calculation easy, we neglect the term of self-shading by phytoplankton in the estimation, because a higher self-shading parameter has the same effect as an increasing light attenuation coefficient by water. The estimated and observed values of these parameters are listed at Table 2. All these parameters estimated are in a reasonable range, although there are some discrepancies compared with observations. In fact, this is not surprising, considering that we assume a single phytoplankton group and neglect the microbial loop and the dynamics of the dissolved organic matter and detritus pools.

## 5 Summary

We have presented a theoretical framework to investigate the interaction of phytoplankton and nutrient in stratified water column. A piecewise function for chlorophyll profiles comprising a linear function in the surface mixed layer and a Gaussian function below is assumed in the nutrient-phytoplankton model at steady state. A number of important findings are obtained.

In steady state, the nitracline is confined between two depths where the gross



665 growth rate equals the recycling rate of dead phytoplankton, indicating that within the  
nitracline, nitrate consumption by phytoplankton has to be replenished by the upward  
flux of nitrate. This layer thereby is the major contributor to NPP.

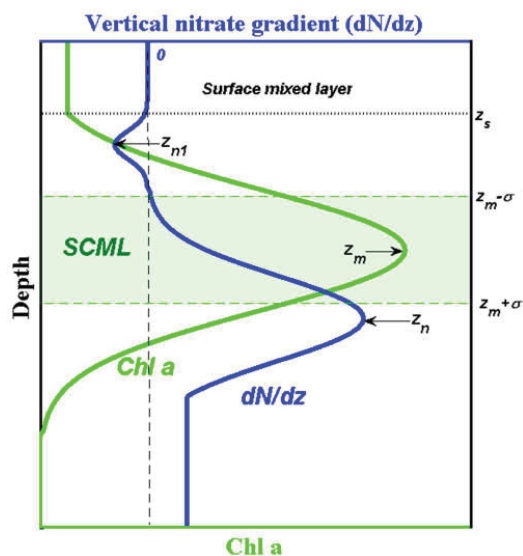
The nitracline depth always locates below the SCML depth, meanwhile, both  
depths deepened as the relaxation of the light limitation (decreasing light attenuation  
670 coefficient or increasing surface light intensity). The nitracline depth does not depend  
on the value of the subsurface diffusivity. The nitracline is steeper with a thinner  
SCML. The nitracline steepness is positively influenced by the light attenuation  
coefficient, yet, responds insignificantly to surface light intensity.

Our analytical solutions show that phytoplankton in the SCML acts as an efficient  
675 nutrient trap, filtering out the upward nitrate supply. The light level at the nitracline  
depth has a positive relation with the maximum rate of NPP and with the  
depth-integrated chlorophyll concentration in the whole water column, acting as the  
indicator of integrated NPP.

**Acknowledgements.** The authors thank State Key Laboratory of Marine  
680 Environmental Science, Xiamen University for providing ISUS nitrate and CTD data,  
especially acknowledge C. J. Du. We are very grateful to the anonymous review for  
the helpful suggestions. We also would like to thank Xiaohuan Liu and Yang Yu for  
valuable advice and programming assistance. This work is funded in part by the  
National Key Basic Research Program of China 2014CB953700, and the National  
685 Nature Science Foundation of China (41406010, 41210008, and 91328202).



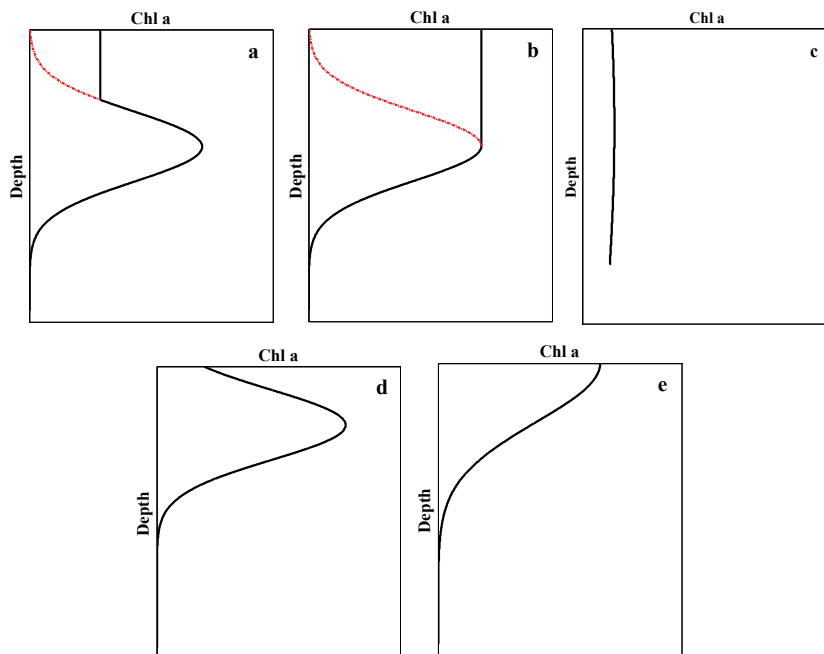
Figures  
 Figure 1



690 Fig. 1 Schematic picture of vertical profiles of nitrate gradient and chlorophyll (Chl a) in stratified  
 water columns. (blue solid line is the vertical profile of nitrate gradient; green solid line is Chl a  
 concentration as a function of depth; red solid line represents the growth limitation by light, red  
 dotted line by nitrate; horizontal green solid lines indicate the locations of the upper and lower  
 SCML,  $z_m - \sigma$ ,  $z_m + \sigma$ , respectively; horizontal black dotted line indicates the depth of the surface  
 mixed layer,  $z_s$ ; vertical dotted black line represents zero nitrate gradient;  $z_{n1}$  and  $z_n$  are the  
 695 locations of extreme nitrate gradients,  $z_n$  is the nitracline depth, and  $z_m$  is the depth of maximum  
 chlorophyll concentration)



Figure 2



700

Fig. 2 Examples of the vertical profiles of chlorophyll (black solid line). (red dotted lines represent the parts of Gaussian fitting curves, not the actual chlorophyll)



Figure 3

705

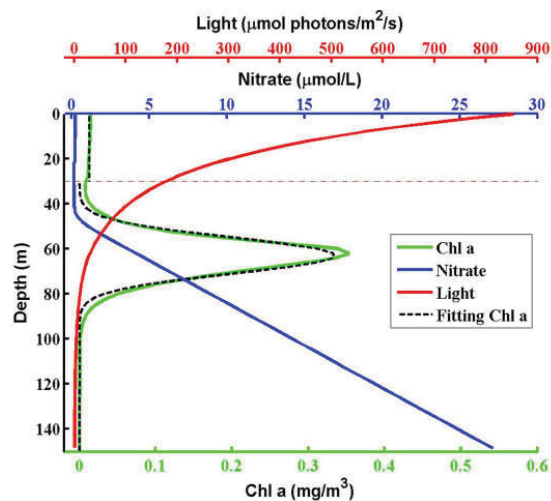


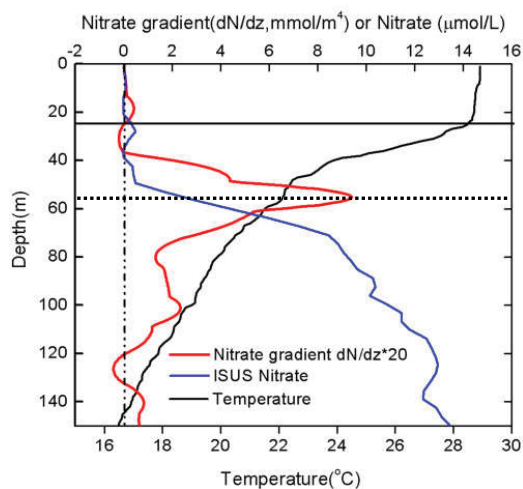
Fig. 3 Steady-state vertical distributions of chlorophyll, nitrate, and light determined by numerical solutions of Eqs. (1) and (2). Horizontal red dash-dotted line indicates the depth of the surface mixed layer. Black dash line represents the fitting curve of vertical chl a profile. The fitting

710 equation is

$$P = \begin{cases} 0.013 & 0 \leq z \leq 30 \\ 0.33 \exp\left[-\frac{(z-63)^2}{2 \times 9^2}\right] & 30 < z < 200 \end{cases}$$



Figure 4



715 Fig. 4 Vertical nitrate gradient, ISUS nitrate and temperature at SEATS station (2012, cast 36)  
(horizontal line indicates the depth of the surface mixed layer, horizontal dotted line indicates the  
depth of nitracline, and the vertical dash-dotted line represents zero nitrate gradient).



Table

Table 1 List of symbols and their values used in models at SEATS station in northern SCS

Model parameters	Description (unit)	Values (range)
$I_0$	Surface light intensity ( $\mu\text{mol photons m}^{-2} \text{s}^{-1}$ )	900 (200-1700) <sup>(1, 2)</sup>
$K_w$	Light attenuation coefficient of water ( $\text{m}^{-1}$ )	0.052 <sup>(1, 3)</sup>
$K_c$	Light attenuation coefficient of phytoplankton ( $\text{m}^2 (\text{mmolN})^{-1}$ )	0.05 <sup>(1, 3)</sup>
$K_I$	Half-saturation constant of light limited growth ( $\mu\text{mol photons m}^{-2} \text{s}^{-1}$ )	40 <sup>(4)</sup>
$K_{v1}$	Surface diffusivity ( $(\times 10^{-4}) \text{m}^2 \text{s}^{-1}$ )	2 <sup>(5)</sup>
$K_{v2}$	Subsurface diffusivity ( $(\times 10^{-5}) \text{m}^2 \text{s}^{-1}$ )	5 <sup>(5)</sup>
$w$	Sinking velocity of phytoplankton ( $\text{m d}^{-1}$ )	1 <sup>(6)</sup>
$\varepsilon$	Loss rate of phytoplankton ( $\text{d}^{-1}$ )	0.3 <sup>(7)</sup>
$\alpha$	Nutrient recycling coefficient (dimensionless)	0.6 <sup>(7)</sup>
$K_N$	Half-saturation constant of nutrient uptake ( $\text{mmol N m}^{-3}$ )	0.4 <sup>(8)</sup>
$\mu_m$	Maximum growth rate of phytoplankton ( $\text{d}^{-1}$ )	0.9 <sup>(5, 7)</sup>
$N_{inML}$	Mixed layer nitrate input ( $(\times 10^{-7}) \text{mmol N m}^{-2} \text{s}^{-1}$ )	4 <sup>(9, 10)</sup>
$\gamma$	Nitrate content of phytoplankton ( $\text{mg chlorophyll per mmol N}$ )	1.59 <sup>(11, 12)</sup>
$\lambda$	Proportion of integrated chlorophyll below surface mixed layer	0.9
$z_s$	Depth of surface mixed layer ( $\text{m}$ )	30 (10-80) <sup>(13, 14)</sup>
$z_b$	Bottom boundary of model domain ( $\text{m}$ )	200
$\frac{dN}{dz} \Big _{z=z_b}$	Nitrate gradient at the bottom boundary of model domain ( $\text{mmol N m}^{-4}$ )	0.2 (0-0.2) <sup>(15, 16, 17)</sup>





Superscripts refer to the references that provide the source for the parameter value and the citations are as follows: <sup>(1)</sup><http://oceandata.sci.gsfc.nasa.gov/SeaWiFS/Mapped/Annual/9km/>;  
720 <sup>(2)</sup>Wu and Gao, 2011; <sup>(3)</sup>Lee Chen et al., 2005; <sup>(4)</sup>Raven and Richardson, 1986; <sup>(5)</sup>Lu et al., 2010;  
<sup>(6)</sup>Bienfang and Harrison, 1984; <sup>(7)</sup>Liu et al., 2007; <sup>(8)</sup>Eppley et al., 1969; <sup>(9)</sup>Kim et al., 2014;  
<sup>(10)</sup>Duce et al., 2008; <sup>(11)</sup>Cloern et al., 1995; <sup>(12)</sup>Oschlies, 2001; <sup>(13)</sup>Wong et al., 2002; <sup>(14)</sup>Tseng et al., 2005; <sup>(15)</sup>Chen et al., 2006; <sup>(16)</sup>Our observations; <sup>(17)</sup>Li et al., 2015.



Table 2 Estimated results and observed values at SEATS station

Variables	Estimated results	Observations
Nitracline depth (m)	79	20-90 <sup>(1, 2, 3)</sup>
Nitracline steepness ( $mmol N m^{-4}$ )	0.24	0.30-0.50 <sup>(3)</sup>
Depth of SCML (m)	59	10-75 <sup>(4, 5, 6)</sup>
Intensity of SCML ( $mg m^{-3}$ )	0.56	0.40-0.90 <sup>(4, 5, 6)</sup>
Thickness of SCML (m)	20	10-55 <sup>(4, 5, 6)</sup>

725 Superscripts refer to the references that provide the source for the parameter value and the citations are as follows: <sup>(1)</sup>Tseng et al., 2005; <sup>(2)</sup>Wong et al., 2007; <sup>(3)</sup>Our observations; <sup>(4)</sup>Chen et al., 2006; <sup>(5)</sup>Liu et al., 2002; <sup>(6)</sup>Liu et al., 2007.



## References:

- 730 Aksnes, D. L., Ohman, M. D., Pascal, R.: Optical effect on the nitracline in a coastal upwelling area, *Limnol. Oceanogr.*, 3, 1179-1187, 2007.
- Anderson, G. C.: Subsurface chlorophyll maximum in the northeast Pacific Ocean, *Limnol. Oceanogr.*, 14, 386-391, 1969.
- 735 Ardyna, M., Babin, M., Gosselin, M., Devred, E., Bélanger, S., Matsuoka, A., Tremblay, J. É.: Parameterization of vertical chlorophyll a in the Arctic Ocean: impact of the subsurface chlorophyll maximum on regional, seasonal, and annual primary production estimates, *Biogeosciences*, 10, 4383-4404, doi:10.5194/bg-10-4383-2013, 2013.
- Bahamón, N., Velásquez, Z., Cruzado, A.: Chlorophyll a and nitrogen flux in the tropical North Atlantic Ocean, *Deep-Sea Res. Pt. I*, 50, 1189-1203, 2003.
- 740 Bahamón, N., Cruzado, A.: Modelling nitrogen fluxes in oligotrophic environments: NW Mediterranean and NE Atlantic, *Ecol. Model.*, 163, 223-244, 2003.
- Banse, K.: Cell volumes, maximal growth rates of unicellular algae and ciliates, and the role of ciliates in the marine pelagial, *Limnol. Oceanogr.*, 27, 1059-1071, 1982.
- 745 Beckmann, A., Hense, I.: Beneath the surface: Characteristics of oceanic ecosystems under weak mixing conditions-A theoretical investigation, *Prog. Oceanogr.*, 75, 771-796, 2007.
- Bienfang, P. K., Harrison, P. J.: Sinking-rate response of natural assemblages of temperate and subtropical phytoplankton to nutrient depletion, *Mar. Biol.*, 83, 293-300, 1984.
- Cermeno, P., Dutkiewicz, S., Harris, R. P., Follows, M., Schofield, O., Falkowski, P. G.: The role of nutricline depth in regulating the ocean carbon cycle., *P. Natl. Acad. Sci. Usa.*, 105, 20344-20349, 2008.
- 750 Chavez, F. P., Messié, M., Pennington, J. T.: Marine primary production in relation to climate variability and change, *Annu. Rev. Mar. Sci.*, 3, 227-260, 2011.
- Cloern, J. E., Grenz, C., Videgar-Lucas, L.: An empirical model of the phytoplankton chlorophyll: carbon ratio-the conservation factor between productivity and growth rate, *Limnol. Oceanogr.*, 40, 1313-1321, 1995.
- Cullen, J. J.: The deep chlorophyll maximum: comparing vertical profiles of chlorophyll a, *Can. J. Fish Aquat. Sci.*, 39, 791-803, 1982.
- Cullen, J. J., Eppley, R. W.: Chlorophyll maximum layers of the Southern California Bight and possible mechanisms of their formation and maintenance, *Oceanol. Acta*, 1, 23-32, 1981.
- 760 Cullen, J. J.: Subsurface Chlorophyll Maximum Layers: Enduring Enigma or Mystery Solved? *Annu. Rev. Mar. Sci.*, 7, 207-239, 2015.
- Denman, K. L., Gargett, A. E.: Time and space scales of vertical mixing and advection of phytoplankton in the upper ocean, *Limnol. Oceanogr.*, 28, 801-815, 1983.
- 765 Du, Y., Mei, L.: On a nonlocal reaction - diffusion - advection equation modelling phytoplankton dynamics, *Nonlinearity*, 24, 319, 2011.
- Du, Y., Hsu, S. B.: On a Nonlocal Reaction-Diffusion Problem Arising from the Modeling of Phytoplankton Growth., *Siam. J. math. anal.*, 42, 1305-1333, 2010.



- 770 Du, Y., Hsu, S. B.: Concentration Phenomena in a Nonlocal Quasi-linear Problem Modelling  
 Phytoplankton I: Existence, *Siam J. Math. Anal.*, 40, 1419-1448, 2008a.
- Du, Y., Hsu, S. B.: Concentration phenomena in a nonlocal quasilinear problem modelling  
 phytoplankton II: Limiting profile, *Siam. J. Math. Anal.*, 40, 1441-1470, 2008b.
- 775 Duce, R. A., Laroche, J., Altieri, K., Arrigo, K. R., Baker, A. R., Capone, D. G., Cornell, S., Dentener,  
 F., Galloway, J., Ganeshram, R. S.: Impacts of atmospheric anthropogenic nitrogen on the open ocean.,  
*Science*, 320, 893-897, 2008.
- Eppley, R. W., Sapienza, C., Renger, E. H.: Gradients in phytoplankton stocks and nutrients off  
 southern California in 1974-76, *Estuar. Coast. Mar. sci.*, 7, 291-301, 1978.
- Eppley, R. W., Renger, E. H., Harrison, W. G.: Nitrate and phytoplankton production in southern  
 California coastal waters, *Limnol. Oceanogr.*, 24, 483-494, 1979.
- 780 Eppley, R. W., Rogers, J. N., McCarthy, J. J.: Half-saturation constant for uptake of nitrate and  
 ammonium by marine phytoplankton, *Limnol. Oceanogr.*, 14, 912-920, 1969.
- Falkowski, P. G., Barber, R. T., Smetacek, V.: Biogeochemical controls and feedbacks on ocean  
 primary production, *Science*, 281, 200, 1998.
- 785 Fennel, K., Boss, E.: Subsurface maxima of phytoplankton and chlorophyll: Steady-state solutions  
 from a simple model, *Limnol. Oceanogr.*, 48, 1521-1534, 2003.
- Fernand, L., Weston, K., Morris, T., Greenwood, N., Brown, J., Jickells, T.: The contribution of the  
 deep chlorophyll maximum to primary production in a seasonally stratified shelf sea, the North Sea,  
*Biogeochemistry*, 1-14, 2013.
- 790 Gong, X., Shi, J., Gao, H. W., Yao, X. H.: Steady-state solutions for subsurface chlorophyll maximum  
 in stratified water columns with a bell-shaped vertical profile of chlorophyll, *Biogeosciences*, 12,  
 905-919, doi:10.5194/bg-12-905-2015, 2015.
- Gong, X., Shi, J., Gao, H.: Modeling seasonal variations of subsurface chlorophyll maximum in South  
 China Sea, *J. Ocean U. China*, 13, 561-571, 2014.
- 795 Herbrand, A., Voituriez, B.: Hydrological structure analysis for estimating the primary production in  
 the tropical Atlantic Ocean, *J. Mar. Res.*, 37, 87-101, 1979.
- Hickman, A. E., Moore, C., Sharples, J., Lucas, M. I., Tilstone, G. H., Krivtsov, V., Holligan, P. M.:  
 Primary production and nitrate uptake within the seasonal thermocline of a stratified shelf sea, *Mar.  
 Ecol. Prog. Ser.*, 463, 39-57, 2012.
- 800 Hodges, B. A., Rudnick, D. L.: Simple models of steady deep maxima in chlorophyll and biomass,  
*Deep-Sea Res. Pt. I*, 51, 999-1015, 2004.
- Hsu, S. B., Yuan, L.: Single Phytoplankton Species Growth with Light and Advection in a Water  
 Column, *Siam. J. Appl. Math.*, 70, 2942-2974, 2010.
- Huisman, J., Thi, N., Karl, D. M., Sommeijer, B.: Reduced mixing generates oscillations and chaos in  
 the oceanic deep chlorophyll maximum, *Nature*, 439, 322-325, 2006.
- 805 Jamart, B. M., Winter, D. F., Banse, K., Anderson, G. C., Lam, R. K.: A theoretical study of  
 phytoplankton growth and nutrient distribution in the Pacific Ocean off the northwestern US coast,  
*Deep-Sea Res.*, 24, 753-773, 1977.
- Jamart, B. M., Winter, D. F., Banse, K.: Sensitivity analysis of a mathematical model of phytoplankton  
 growth and nutrient distribution in the Pacific Ocean off the northwestern US coast, *J. Plankton Res.*, 1,  
 810 267-290, 1979.



- Johnson, K. S., Coletti, L. J.: In situ ultraviolet spectrophotometry for high resolution and long-term monitoring of nitrate, bromide and bisulfide in the ocean, *Deep-Sea Res. Pt. I*, 49, 1291-1305, 2002.
- Johnson, K. S., Riser, S. C., Karl, D. M.: Nitrate supply from deep to near-surface waters of the North Pacific subtropical gyre, *Nature*, 465, 1062-1065, 2010.
- 815 Katsumi, H., Hitomi, K.: Vertical Nutrient Distributions in the Western North Pacific Ocean: Simple Model for Estimating Nutrient Upwelling, Export Flux and Consumption Rates, *J. Oceanogr.*, 59, 149-161, 2003.
- Kiefer, D. A., Kremer, J. N.: Origins of vertical patterns of phytoplankton and nutrients in the temperate, open ocean: a stratigraphic hypothesis, *Deep-Sea Res. Pt. I*, 28, 1087-1105, 1981.
- 820 Kim, T. W., Lee, K., Duce, R., Liss, P.: Impact of atmospheric nitrogen deposition on phytoplankton productivity in the South China Sea, *Geophys. Res. Lett.*, 41, 3156-3162, 2014.
- Klausmeier, C. A., Litchman, E.: Algal games: The vertical distribution of phytoplankton in poorly mixed water columns, *Limnol. Oceanogr.*, 8, 1998-2007, 2001.
- Koeve, W., Eppley, R. W., Podewski, S., Zeitzschel, B.: An unexpected nitrate distribution in the tropical North Atlantic at 18° N, 30° W—implications for new production, *Deep-Sea Res. Pt. II*, 40, 521-536, 1993.
- 825 Laanemets, J., Kononen, K., Pavelson, J., Poutanen, E. L.: Vertical location of seasonal nutriclines in the western Gulf of Finland, *J. Marine Syst.*, 52, 1-13, 2004.
- Lande, R., Li, W. K. W., Horne, E. P. W., Wood, A. M.: Phytoplankton growth rates estimated from depth profiles of cell concentration and turbulent diffusion, *Deep-Sea Res. Pt. A. Oceanographic Research Papers*, 36, 1141-1159, 1989.
- 830 Lande, R., Wood, A. M.: Suspension times of particles in the upper ocean, *Deep-Sea Res. Pt. A. Oceanographic Research Papers*, 34, 61-72, 1987.
- Lavigne, H., D'Ortenzio, F., Ribera D'Alcalà, M., Claustre, H., Sauzède, R., Gacic, M.: On the vertical distribution of the chlorophyll a concentration in the Mediterranean Sea: a basin scale and seasonal approach, *Biogeosciences*, 12, 5021-5039, doi:10.5194/bg-12-5021-2015, 2015.
- Lee Chen, Y.: Spatial and seasonal variations of nitrate-based new production and primary production in the South China Sea, *Deep Sea Research Part I: Oceanographic Research Papers*, 52, 319-340, 2005.
- 840 Letelier, R. M., Karl, D. M., Abbott, M. R., Bidigare, R. R.: Light driven seasonal patterns of chlorophyll and nitrate in the lower euphotic zone of the North Pacific Subtropical Gyre, *Limnol. Oceanogr.*, 49, 508-519, 2004.
- Lewis, M. R., Harrison, W. G., Oakey, N. S., Hebert, D., Platt, T.: Vertical nitrate fluxes in the oligotrophic ocean, *Science*, 234, 870-873, 1986.
- 845 Lewis, M. R., Cullen, J. J., Platt, T.: Phytoplankton and thermal structure in the upper ocean: consequences of nonuniformity in chlorophyll profile, *J. Geophys. Res.*, 88, 2565-2570, 1983.
- Li, Q. P., Wang, Y., Dong, Y., Gan, J.: Modeling long - term change of planktonic ecosystems in the northern South China Sea and the upstream Kuroshio Current, *J. Geophys. Res. Oceans*, 120, 3913–3936, 2015.
- Lipschultz, F., Bates, N. R., Carlson, C. A., Hansell, D. A.: New production in the Sargasso Sea: History and current status, *Global Biogeochem. Cy.*, 16, 1, 1001, 10.1029/2000GB001319, 2002.
- 850 Liu, K. K., Chao, S. Y., Shaw, P. T., Gong, G. C., Chen, C. C., Tang, T. Y.: Monsoon-forced chlorophyll distribution and primary production in the South China Sea: observations and a numerical



- study, *Deep-Sea Res. Pt. I*, 49, 1387-1412, 2002.
- Liu, K. K., Chen, Y. J., Tseng, C. M., Lin, I. I., Liu, H. B., Snidvongs, A.: The significance of phytoplankton photo-adaptation and benthic-pelagic coupling to primary production in the South China Sea: Observations and numerical investigations, *Deep-Sea Res. Pt. II*, 2007, 1546-1574, 2007.
- 855 Lu, Z., Gan, J., Dai, M., Cheung, A.: The influence of coastal upwelling and a river plume on the subsurface chlorophyll maximum over the shelf of the northeastern South China Sea, *J. Marine Syst.*, 82, 35-46, 2010.
- 860 Lund-Hansen, L. C.: Subsurface chlorophyll maximum (SCM) location and extension in the water column as governed by a density interface in the strongly stratified Kattegat estuary, *Hydrobiologia*, 1-14, 2011.
- Mackey, K. R. M., van Dijken, G. L., Mazloom, S., Erhardt, A. M., Ryan, J., Arrigo, K. R., Paytan, A.: Influence of atmospheric nutrients on primary productivity in a coastal upwelling region, *Global Biogeochem Cy.*, 24, B4027, 2010.
- 865 Martin, A. P., Pondaven, P.: On estimates for the vertical nitrate flux due to eddy pumping, *J. Geophys. Res.* (1978 - 2012), 108, C11, 3359, 2003.
- Martin, J., Tremblay, J. É., Price, N. M.: Nutritive and photosynthetic ecology of subsurface chlorophyll maxima in Canadian Arctic waters, *Biogeosciences*, 9, 5353-5371, doi:10.5194/bg-9-5353-2012, 2012.
- 870 Martin, J., Tremblay, J., Gagnon, J., Tremblay, G., Lapoussière, A., Jose, C., Poulin, M., Gosselin, M., Gratton, Y., Michel, C.: Prevalence, structure and properties of subsurface chlorophyll maxima in Canadian Arctic waters, *Mar. Ecol. Prog. Ser.*, 412, 69-84, 2010.
- 875 Matsumura, S., Shiimoto, A.: Vertical distribution of primary productivity function F (II) for the estimation of primary productivity using by satellite remote sensing, *Bull. Nat. Res. Inst. Far Seas Fish.*, 30, 227-270, 1993.
- Mellard, J. P., Yoshiyama, K., Litchman, E., Klausmeier, C. A.: The vertical distribution of phytoplankton in stratified water columns, *J. Theor. Biol.*, 269, 16-30, 2011.
- 880 Mellard, J. P., Yoshiyama, K., Klausmeier, C. A., Litchman, E.: Experimental test of phytoplankton competition for nutrients and light in poorly mixed water columns, *Ecol. Monogr.*, 82, 239-256, 2012.
- Mignot, A., Claustre, H., D'Ortenzio, F., Xing, X., Poteau, A., Ras, J.: From the shape of the vertical profile of in vivo fluorescence to Chlorophyll-a concentration, *Biogeosciences*, 8, 2391-2406, doi:10.5194/bg-8-2391-2011, 2011.
- 885 Mu Oz Anderson, M., Hernández Walls, R., Rojas Mayoral, E., Galindo Bect, S.: Fitting vertical chlorophyll profiles in the California Current using two Gaussian curves, *Limnol. Oceanogr. Methods* 00, doi: 10.1002/lom3.10034, 2015.
- Navarro, G., Ruiz, J.: Hysteresis conditions the vertical position of deep chlorophyll maximum in the temperate ocean, *Global Biogeochem Cy.*, 1-10, 2013.
- 890 Okin, G. S., Baker, A. R., Tegen, I., Mahowald, N. M., Dentener, F. J., Duce, R. A., Galloway, J. N., Hunter, K., Kanakidou, M., Kubilay, N., Prospero, J. M., Sarin, M., Surapipith, V., Uematsu, M., Zhu, T.: Impacts of atmospheric nutrient deposition on marine productivity: Roles of nitrogen, phosphorus, and iron, *Global Biogeochem Cy.*, 25, B2022, 2011.
- Omand, M. M., Mahadevan, A.: The shape of the oceanic nitracline, *Biogeosciences*, 12, 3273-3287, doi:10.5194/bg-12-3273-2015, 2015.



- 895 Oschlies, A.: Model-derived estimates of new production: New results point towards lower values, *Deep-Sea Res. Pt. II*, 48, 2173-2197, 2001.
- Parsons, T. R., Maita, Y., Lalli, C. M., 1984. A manual of chemical and biological methods for seawater analysis, xiv + 173 pp. Oxford: Pergamon Press.
- Platt, T., Sathyendranath, S., Caverhill, C. M., Lewis, M. R.: Ocean primary production and available  
 900 light: further algorithms for remote sensing, *Deep-Sea Res. Pt. I*, 35, 855-879, 1988.
- Probyn, T. A., Mitchell-Innes, B. A., Searson, S.: Primary productivity and nitrogen uptake in the subsurface chlorophyll maximum on the Eastern Agulhas Bank, *Cont. Shelf Res.*, 15, 1903-1920, 1995.
- Richardson, T. L., Cullen, J. J.: Changes in buoyancy and chemical composition during growth of a coastal marine diatom: Ecological and biogeochemical consequences, *Mar. Eco. Prog.*, 128, 77-90,  
 905 1995.
- Raven, J. A. and Richardson K.: Photosynthesis in marine environments. In: *Topics in Photosynthesis*, Elsevier, edited by: Baker, N. R. and Long, S., 7, 337-399, 1986.
- Riley, G. A., Stommel, H., Bumpus, D. F.: Quantitative ecology of the plankton of the western North Atlantic, *Bulletin Bingham Oceanogr. Collect.*, 12, 1-69, 1949.
- 910 Ross, O. N., Sharples, J.: Phytoplankton motility and the competition for nutrients in the thermocline, *Mar. Ecol. Prog. Ser.*, 347, 21-38, 2007.
- Ryabov, A. B., Rudolf, L., Blasius, B.: Vertical distribution and composition of phytoplankton under the influence of an upper mixed layer, *J. Theor. Biol.*, 263, 120-133, 2010.
- Sakamoto, C. M., Johnson, K. S., Coletti, L. J.: Improved algorithm for the computation of nitrate  
 915 concentrations in seawater using an in situ ultraviolet spectrophotometer, *Limnol. Oceanogr.*, 7, 132-143, 2009.
- Sharples, J., Moore, C. M., Rippeth, T. P., Holligan, P. M., Hydes, D. J., Fisher, N. R., Simpson, J. H.: Phytoplankton distribution and survival in the thermocline, *Limnol. Oceanogr.*, 46, 486-496, 2001.
- Shigesada, N., Okubo, A.: Analysis of the self-shading effect on algal vertical distribution in natural  
 920 waters, *J. Math. Biol.*, 12, 311-326, 1981.
- Steele, J. H., Yentsch, C. S.: The vertical distribution of chlorophyll, *J. Mar. Biol. Assoc. UK.*, 39, 217-226, 1960.
- Steele, J. H.: A study of production in the Gulf of Mexico, *J. Mar. Res.*, 22, 211-222, 1964.
- Sverdrup, H. U.: On conditions for the vernal blooming of phytoplankton, *J. Cons. int. Explor. Mer.*, 18,  
 925 287-295, 1953.
- Teira, E., Mourino, B., Marañón, E., Pérez, V., Pazo, M. J., Serret, P., de Armas, D., Escanez, J., Woodward, E., Fernández, E.: Variability of chlorophyll and primary production in the Eastern North Atlantic Subtropical Gyre: potential factors affecting phytoplankton activity, *Deep-Sea Res. Pt. I*, 52, 569-588, 2005.
- 930 Timmermans, K. R., Van der Wagt, B., Veldhuis, M., Maatman, A., De Baar, H.: Physiological responses of three species of marine pico-phytoplankton to ammonium, phosphate, iron and light limitation, *J. Sea Res.*, 53, 109-120, 2005.
- Tseng, C. M., Wong, G. T. F., Lin, I. I., Wu, C. R., Liu, K. K.: A unique seasonal pattern in phytoplankton biomass in low-latitude waters in the South China Sea, *Geophys. Res. Lett.*, 32, L8608, 2005.  
 935
- Uitz, J., Claustre, H., Morel, A., Hooker, S. B.: Vertical distribution of phytoplankton communities in



- open ocean: An assessment based on surface chlorophyll, *J. Geophys. Res.*, 111, C8005, 2006.
- Varela, R. A., Cruzado, A., Tintoré, J.: A simulation analysis of various biological and physical factors influencing the deep-chlorophyll maximum structure in oligotrophic areas, *J. Marine Syst.*, 5, 143-157, 1994.
- 940 Ward, B. B., Kilpatrick, K. A., Renger, E. H., Eppley, R. W.: Biological nitrogen cycling in the nitracline., *Limnol. Oceanogr.*, 34, 493-513, 1989.
- Wong, G. T. F., Shi Wei, C., Fuh Kwo, S., Chen, C. C., Wen, L. S., Liu, K. K.: Nitrate anomaly in the upper nutricline in the northern South China Sea - Evidence for nitrogen fixation, *Geophys. Res. Lett.*, 29, 11-12, 2002.
- 945 Wong, G. T. F., Tseng, C. M., Wen, L. S., Chung, S. W.: Nutrient dynamics and N-anomaly at the SEATS station, *Deep-Sea Res. Pt. II*, 54, 1528-1545, 2007.
- Wu Y. P. and Gao K. S.: Photosynthetic response of surface water phytoplankton assemblages to different wavebands of UV radiation in the South China Sea, *Acta Oceanol. Sin.*, 5, 146-151, 2011.
- 950 Xiu, P., Liu, Y., Tang, J.: Variations of ocean colour parameters with nonuniform vertical profiles of chlorophyll concentration, *Int J. Remote Sens.*, 29, 831-850, 2008.
- Yoshiyama, K., Nakajima, H.: Catastrophic transition in vertical distributions of phytoplankton: Alternative equilibria in a water column, *J. Theor. Biol.*, 216, 397-408, 2002.